Metallogr. Microstruct. Anal. (2017) 6:541–552
https://doi.org/10.1007/s13632-017-0395-0

TECHNICAL ARTICLE

Microstructural and Mechanical Characterization of CNT- and Al_2O_3-Reinforced Aluminum Matrix Nanocomposites Prepared by Powder Metallurgy Route

Meysam Toozandehjani[1] · **Farhad Ostovan**[2]

Received: 10 June 2017 / Revised: 27 September 2017 / Accepted: 15 October 2017 / Published online: 20 November 2017

Abstract In this work, carbon nanotube (CNT) and alumina (Al_2O_3) nanoparticles have been incorporated into the pure aluminum (Al) matrix using ball milling as a part of powder metallurgy route. The benefits and limitations of addition of different amounts of CNT and Al_2O_3 nanoparticles into pure aluminum matrix have been investigated. Different amounts of CNT and Al_2O_3 nanoparticles were dispersed into pure Al matrix using ball milling at different times from 0.5 h up to 12 h. Composite powders were consolidated by uniaxial cold pressing at a pressure of 150 MPa followed by sintering at 530 °C under argon atmosphere. From microstructural point of view, ball milling was found to be an effective method for dispersion of CNT and Al_2O_3 nanoparticles within pure aluminum matrix. It should be noted that there is limitation when a large weigh fraction of CNTs is used. It was found that the threshold of CNTs is 2 wt.%; however, up to 10 wt.% of Al_2O_3 nanoparticles can be used. Most of Al-CNT and Al-Al_2O_3 nanocomposites were found to reach steady state after 8 of milling except Al-5CNT and Al-10CNTs which never reached steady state due to the formation of big agglomerates resulting in non-homogenous nanocomposite powders. Young's modulus and hardness of Al-CNT nanocomposites were found to be higher than Al-Al_2O_3 nanocomposites, while a homogenous dispersion of reinforcements within matrix was observed.

Keywords Aluminum matrix nanocomposites · Ball milling · Powder metallurgy · Microstructure · Mechanical properties

Introduction

Aluminum matrix composites (AMCs) have attracted more attention in aerospace, automotive, and military industries due to their outstanding mechanical properties including high strength-to-weight ratio, good wear resistance, good environmental resistance as well as lower costs of production [1–4].

Owing to the unique properties of Al_2O_3 and CNT nanoparticles, they have incorporated into aluminum matrix as a reinforcement to fabricate Al-Al_2O_3 [5–8] and Al-CNT [9–13] nanocomposites. Addition of even small amount of these nanoparticle reinforcements provides effective improvement of the physical and mechanical behavior of those nanocomposites. Incorporating of CNT and Al_2O_3 nanoparticles into aluminum matrix is difficult task particularly when a larger content of these nanoparticles is used. As a matter of fact, dispersion technique of CNTs and Al_2O_3 into aluminum matrix affects their dispersion, morphological and microstructural features of constituents and consequently physical and mechanical behavior of these nanocomposites. It might even negatively influence the mechanical behavior and reduces the mechanical properties of these nanocomposites [14, 15].

Obtaining a homogenous dispersion of CNT and Al_2O_3 nanoparticles within the Al matrix powder, avoiding clustering and agglomeration of the powder mixture, good

✉ Farhad Ostovan
F.ostovan@gmail.com

Meysam Toozandehjani
Toozandejani.meysam@yahoo.com

[1] Materials Synthesis and Characterization Laboratory, Institute of Advanced Technology, Universiti Putra Malaysia, Serdang, Selangor, Malaysia

[2] Department of Material Science and Engineering, Islamic Azad University, Bandarabbas Branch, Bandar Abbas, Iran

interfacial bonding between Al and CNTs and Al_2O_3 and retention of CNTs structure after the consolidation process could be considered as challenges one may face during the production of these nanocomposites [10, 16–18]. Therefore, a powder processing technique to overcome these challenges which mainly dominant within powder processing is required. As a well-known powder processing technique, mechanical alloying through ball milling as a part of powder metallurgy route is proposed to be an effective dealing with these challenges particularly dispersion of CNT and Al_2O_3 nanoparticles [14, 19].

Previously published work in the literature has shown that Al-CNT and Al-Al_2O_3 nanocomposites have been successfully fabricated using a combination of ball milling and power metallurgical consolidation [5, 16, 20, 21]. Different amounts of CNT and Al_2O_3 nanoparticles are incorporated into pure Al matrix, and enhancement of mechanical behavior of those nanocomposites has been reported. Therefore, in the current work, the effect of addition of CNT and Al_2O_3 nanoparticles into pure matrix alloys is investigated and compared. The emphasis is on the morphological and microstructural features of Al-CNTs and Al-Al_2O_3 nanocomposite powders during ball milling as a part of powder metallurgy route and its consequent effect on the mechanical behavior of nanocomposites.

Materials and Methods

Flake-shaped pure aluminum powder (99% purity and ~ 200 μm), spherical shape Al_2O_3 nanoparticles (~ 200 nm), and multi-walled CNT powders (~ 20–30 nm of outer diameter and 10–30 mm in length) were used as a raw material to produce Al-CNT and Al-Al_2O_3 nanocomposites. Figure 1 shows the morphology of as-received pure Al, Al_2O_3 nanoparticles, and NTs.

Different amounts of CNT and Al_2O_3 nanoparticles from 1 to 10 wt.% were incorporated into pure Al using a planetary ball milling machine (PM100). Nanocomposite powder mixtures were ball-milled for different times up to 12 h. The ball-to-powder weight ratio (BPR) was 10:1, while the rotational speed of machine was maintained constant at 300 revolutions per minute (rpm). Nanocomposite powders were then consolidated by uniaxial cold pressing at a pressure of 150 MPa followed by sintering at 530 °C for 45 min under argon atmosphere to obtain sound bulk nanocomposite specimens.

Morphology and dispersion uniformity of CNT and Al_2O_3 nanoparticles within pure Al matrix were observed using scanning electron microscopy (SEM), field emission scanning electron microscopy (FESEM), and transmission electron microscopy (TEM). Phase analysis of nanocomposite powders within milling process was performed by x-ray diffractometers (XRD-6000) using 0.1542 nm CuK_α 181 radiation at 4.8 kW with the voltage of 40 kV and a current of 120 mA. Present peaks in the XRD patterns of nanocomposite powders were indexed using Xpert High-score plus software. A Raman spectrometer with an excitation wavelength of 532.200 nm was used to characterize variation of CNTs structure during milling.

Nanoindentation was conducted on the polished cross section of specimens using an indenter equipped with a standard Berkovich geometry tip indenter in order to deduce the nanohardness (HN) and Young's modulus (E) of nanocomposites. A constant loading rate of 0.5 μN/s was applied to the polished surface of specimens until reaching the maximum load of 50 μN. Maximum load was hold for 5 s and then unloaded gradually to zero. Total 20 indents were made at different locations of specimens for each value of the peak load. The average values of HN and E were calculated and reported. The values of HN and E of nanocomposite specimens can be derived according to Oliver–Pharr method according to the following equations [22].

$$H_N = \frac{P_{max}}{A} \quad (1)$$

P_{max} is the peak indentation load and A is the projected contact area under the peak indentation load of the load–displacement curve. The elastic modulus of the nanocomposite specimens can be inferred as:

$$\frac{1}{E_r} = \frac{1-v_s^2}{E_s} + \frac{1-v_i^2}{E_i} \quad (2)$$

E_s and v_s are the elastic modulus and Poisson's ratio of the specimen, respectively. E_s and v_i are the corresponding elastic modulus and Poison's ratio of the Berkovich indenter (E_i = 1040 GPa and v_i = 0.07).

Results and Discussion

It is well-known fact that each reinforcement provides different characteristic profiles, while the same composition and amounts of the reinforcement are being used [15]. In this work, Al_2O_3 nanoparticles and CNTs used are different in shape and intrinsic properties so that the milling process, morphological and microstructural features of powders during and after milling process as well as the mechanical behavior of Al-CNT and Al-Al_2O_3 nanocomposites differ from each other.

Morphology Evolution of Ball-Milled Al-Al_2O_3 and Al-CNT Nanocomposites

Figures 2, 3, 4, and 5 illustrate the morphology of Al-Al_2O_3 and Al-CNTs nanocomposite powders. Different

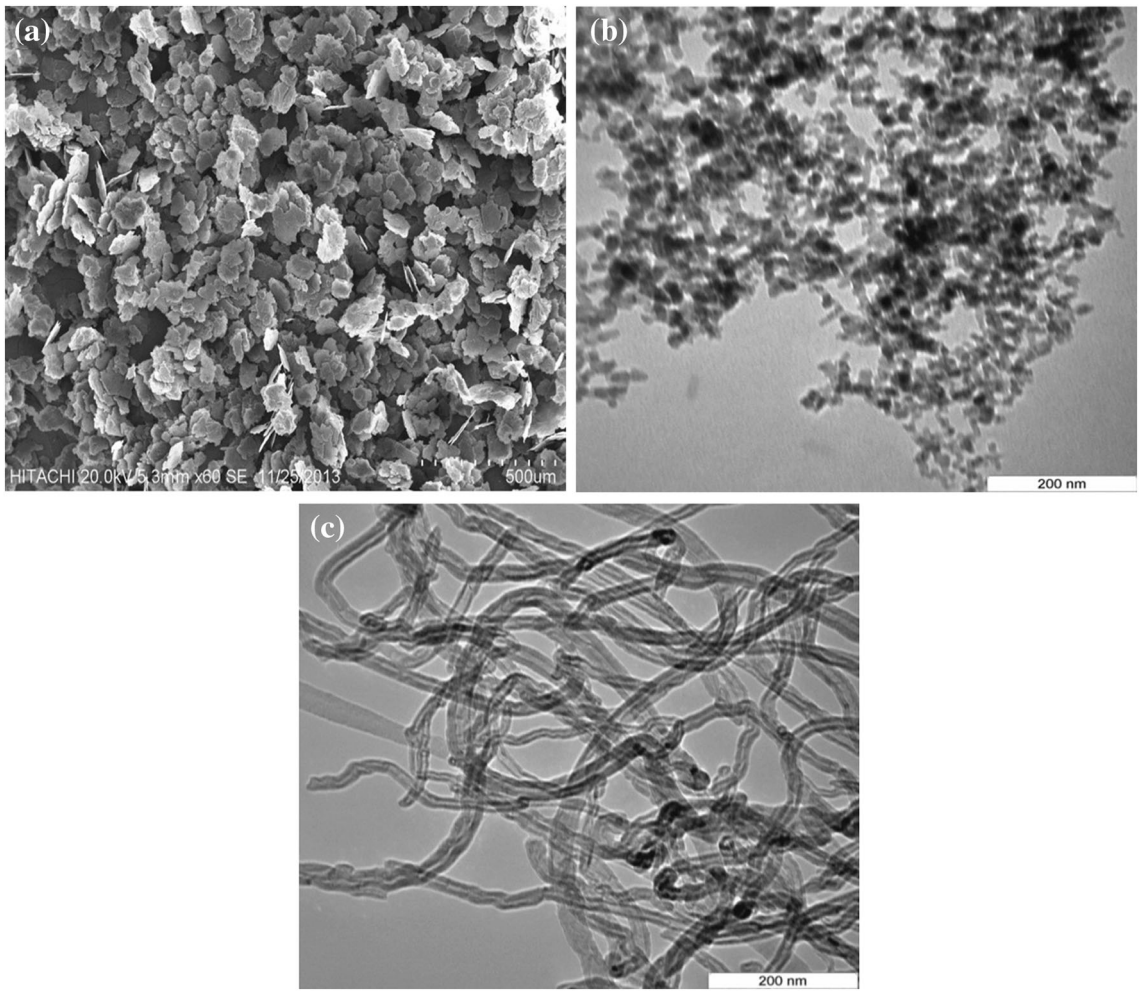

Fig. 1 Morphology of as-received powders (**a**) Pure Al, (**b**) Al_2O_3, and (**c**) CNTs

stages of milling can be observed during milling of both Al-Al_2O_3 and Al-CNT nanocomposites. These stages may include cold welding, fracturing of nanocomposite powders, and steady state [18].

Figure 2 shows the morphology of Al-1 wt.% Al_2O_3 (Al-1Al_2O_3) milled for different milling times up to 12 h. Al-1Al_2O_3 nanocomposite powders milled for short time of 0.5 h are not significantly influenced by milling process. Nanocomposite particles have preserved their initial shapes; however, the ductile Al particles gone under flattening process in some areas. As milling time increases up to 2 h, cold welding mechanism is activated leading to flattening of soft Al particles as a result of a high impact collision of the balls. Lamination of particles is dominant in early stage of milling. Therefore, large flake-shaped particles with large particle size are formed due to the cold welding of particles at early stages of milling up to 2 h. As the milling time proceeds, particles are welded and fractured until reaching a steady state. The presence of reinforcement particles accelerates the milling process by increasing local deformation in the vicinity of the Al particles. Therefore, a considerable change in the morphology of the powders can be observed after 2 h of milling until reaching to a steady state after 8 h of milling (Fig. 2c). After 8 h of milling, the powder particles morphology stabilizes and particles are in an almost equiaxed shape and certain size which randomly oriented which is a characteristic of steady state (Fig. 4d). At prolonged milling time of 12 h, the steady state still predominates and milling has no considerable effect on morphology of the powders; however, grain refinement is expected (Fig. 4e). There is also a similar trend in the variation in morphology of different Al-Al_2O_3 nanocomposites containing different Al_2O_3 contents. In all Al-Al_2O_3 systems, the cold welding and fracture of powder particles are still predominant mechanisms during milling process of powders; however, the plastic deformation is more pronounced. The steady state was found to be appeared at 8 h when large content of Al_2O_3 used (Fig. 3a). However, the efficiency of milling process decreases in Al-10Al_2O_3 nanocomposites where

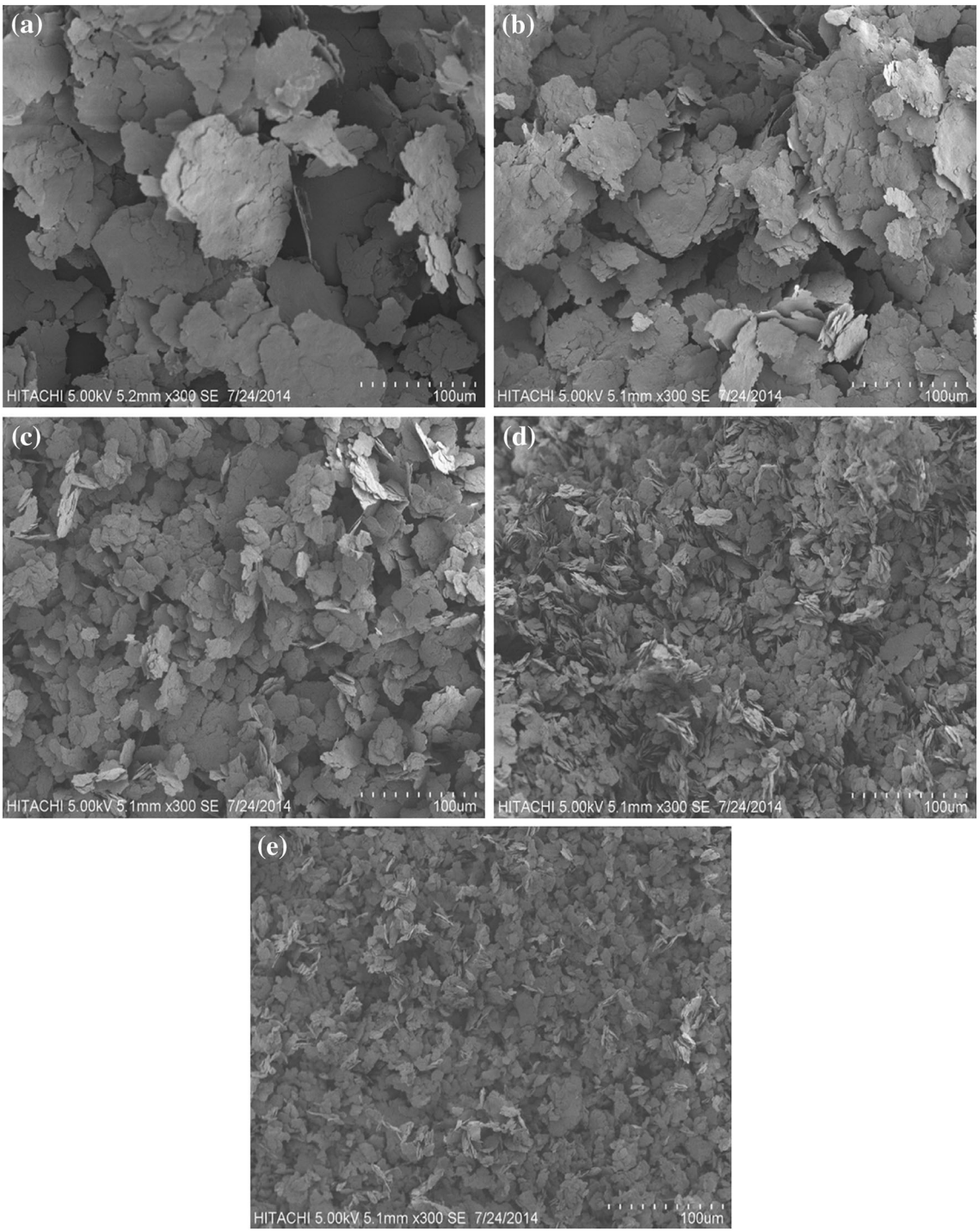

Fig. 2 Morphology of milled Al-1Al_2O_3 nanocomposites for (**a**) 0.5 h, (**b**) 2 h, (**c**) 5 h, (**d**) 8 h, and (**e**) 12 h [5]

some agglomerates were observed in the microstructure (Fig. 3b).

Morphology variation of Al-2 wt.% CNT nanocomposites (Al-2CNTs) milled for various times is shown in Fig. 4. As it is expected, milling time of 0.5 h is quiet short to have significant effect on the morphology of the Al-2CNTs nanocomposite powders. However, partial deformation of nanocomposite particles could be observed, but nanocomposite particles have almost preserved their initial shapes (Fig. 4a). By increasing milling time up to 2 h, more flattening of Al particles is observed due to activation of cold welding mechanism. Flattened particles are welded one over the other one, building a large quasi-laminar morphology. As milling time proceeds up to 8 h,

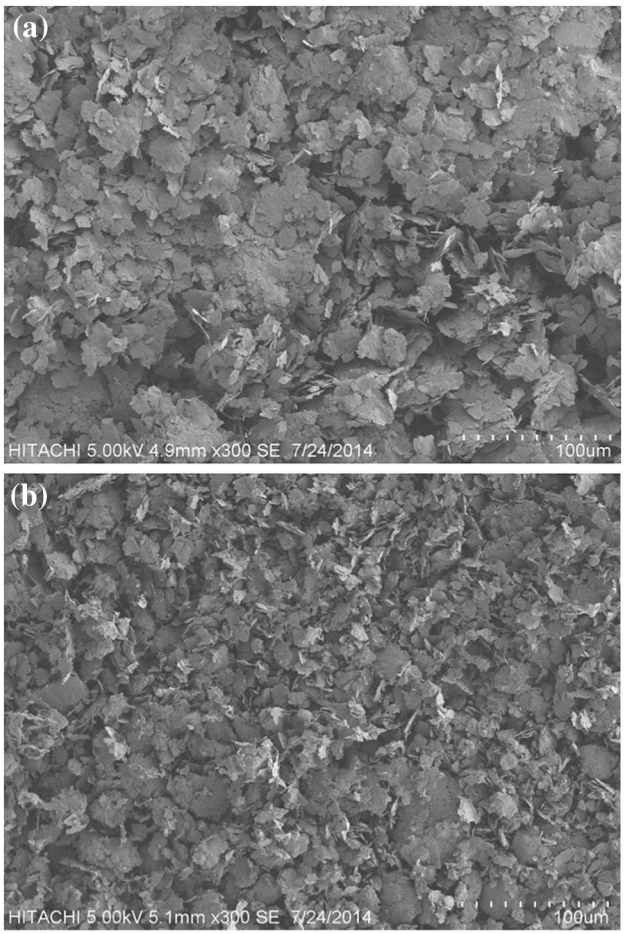

Fig. 3 Morphology of (**a**) Al-5Al_2O_3 and (**b**) Al-10Al_2O_3 nanocomposite powders milled for 8 h

excessive work hardening and increment of brittleness of soft Al powders activate the fracture mechanism. At this stage, brittle and work-hardened Al particles are significantly fractured until reach to a steady state after 8 h of milling where equilibrium between the fracture and cold welding of Al particles is obtained. Fracturing of work-hardened and brittle aluminum powders results in the formation of irregular shape of powders particles with smaller particle size. After 8 h of milling, the powder particles morphology stabilizes and particles are more or less equiaxial with certain size (Fig. 4d). According to Fogagnolo et al. [18], stabilizing the morphology is a characteristic of steady state. Further milling of Al-2CNTs nanocomposite powders up to 12 h results in no considerable change in the morphology of nanocomposite powder particles (Fig. 4e).

Dissimilar to Al-Al_2O_3 nanocomposites, there is different trend in the variation of morphology of Al-CNT powders in the presence of various contents of CNTs. In All Al-CNT systems, the cold welding and fracture of powder particles and steady state are still predominant mechanisms during milling process. However, Al-5CNT and Al-10CNT nanocomposites never reached to steady state since some agglomerates of particles were found in Al-5CNT and Al-10CNT nanocomposite microstructures even at long time of 12 h (Fig. 5). The remaining big agglomerates result in non-homogenous nanocomposite powder microstructure. It seems that Al-5CNT and Al-10CNT need longer time of milling to reach steady state.

Dispersion Uniformity of CNT and Al_2O_3 Nanoparticles within Pure Al Matrix

In order to fully benefit from the gain in mechanical properties in Al-10Al_2O_3 and Al-CNTs, a uniform dispersion of CNTs and Al_2O_3 nanoparticles within pure Al is needed. However, dispersion of CNT and Al_2O_3 nanoparticles within pure Al matrix is a difficult task due to their smaller size than the matrix and their high specific surface area which favor the interaction between nanoparticles. According to Xiong et al. [23], agglomeration and clustering are critical issues associated with nanoscale reinforcements due to the difference in size, physical and chemical properties with respect to the matrix powder.

The dispersion uniformity of Al_2O_3 nanoparticles within the pure Al matrix of Al-2Al_2O_3 and Al-10Al_2O_3 nanocomposites milled for different times is shown in Fig. 6. Generally, as ball milling time increases, the dispersion of Al_2O_3 nanoparticles within the aluminum matrix increases until a well-homogenous dispersion obtains at the steady state after 8 h of milling.

Short milling time of 0.5 h is found to be a simple mixing stage with no considerable effect on the dispersion of Al_2O_3 nanoparticles within the Al matrix. It can be seen that most of Al_2O_3 nanoparticles have mostly been remained clustered on the surfaces of Al particles, while a plenty of surface area of the Al particles is uncovered (Fig. 6a). Dispersion of Al_2O_3 nanoparticles increases with increasing the milling time to 8 h where homogenous dispersion of Al_2O_3 nanoparticles is obtained (Fig. 6b). Al_2O_3 nanoparticles are spread on the surface of the Al particles. It also seems that 8 h of milling is long enough to disperse Al_2O_3 nanoparticles within Al matrix even at larger Al_2O_3 contents. Figure 6c shows the homogenous dispersion of 10 wt.% of Al_2O_3 nanoparticles within Al matrix after 8 h of milling. Milling times longer than 8 h result in no noticeable change in the homogeneous dispersion of Al_2O_3 nanoparticles at steady state.

The dispersion of CNTs within Al matrix was found to be more difficult than Al_2O_3 nanoparticles particularly when a larger content of CNTs is used. Dispersion uniformity of CNTs in Al-2CNTs and Al-5CNTs nanocomposite powders at different milling times is shown in Fig. 7.

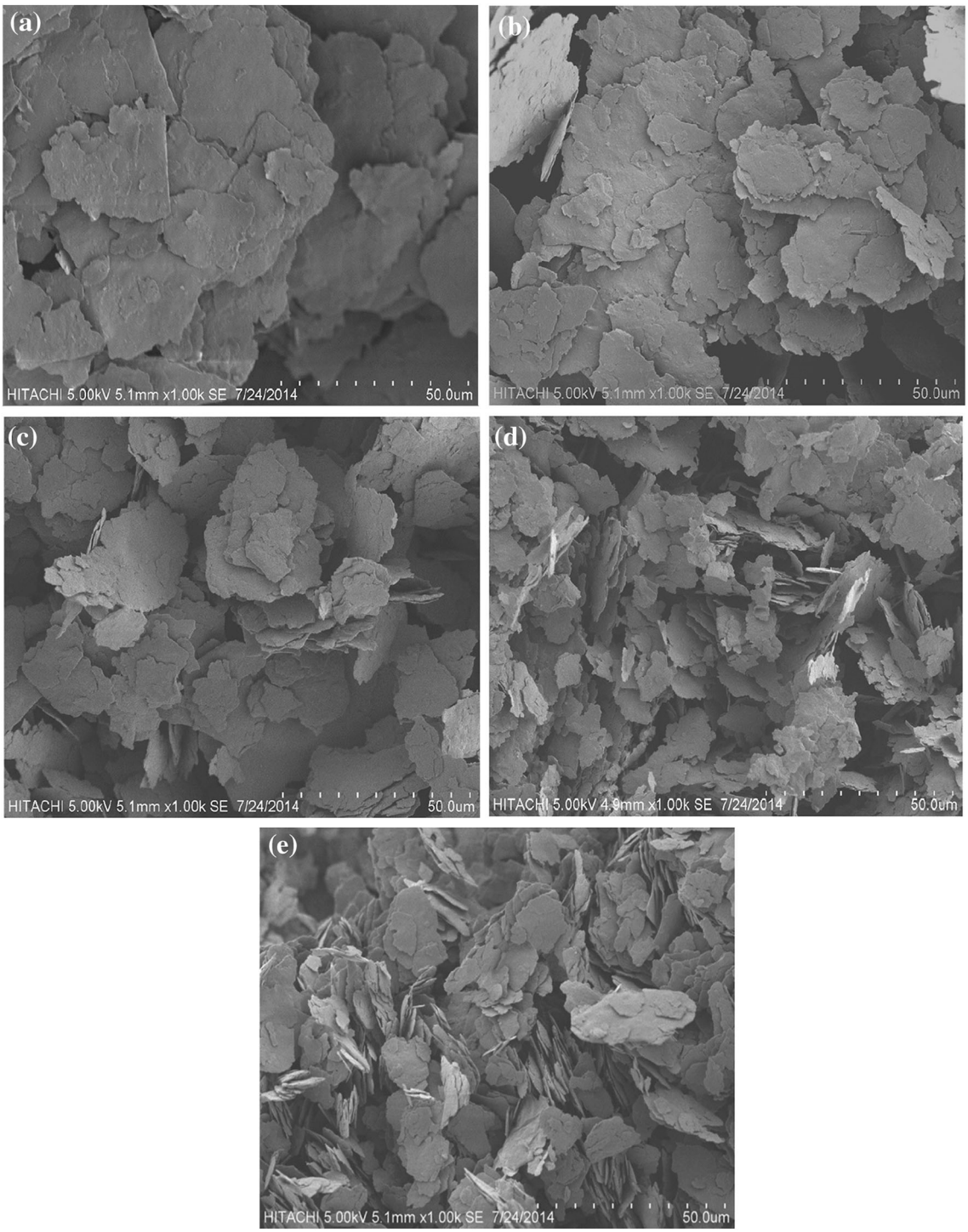

Fig. 4 Morphology of Al-2CNT nanocomposites milled for (**a**) 0.5 h, (**b**) 2 h, (**c**) 5 h, (**d**) 8 h, and (**e**) 12 h

At an early stage of milling up to 2 h, most of the CNTs have preserved their initial shapes and remained clustered. Figure 7a shows the entangled CNT clusters which are located in the grain boundaries. The adhesion of CNTs on the surface of Al particles is not achieved either. By further increasing the milling time, independent clusters of CNTs are effectively broken up and CNTs start to disperse with better homogeneity throughout Al matrix. Due to plastic deformation of particles during milling process, CNTs are also shortened and changed from entangled clusters to open entangled CNTs. CNTs are gradually dispersed within aluminum powder as milling time increases. After 8 h of milling, CNTs are almost dispersed uniformly where Al particles are surrounded by the CNTs, indicating the

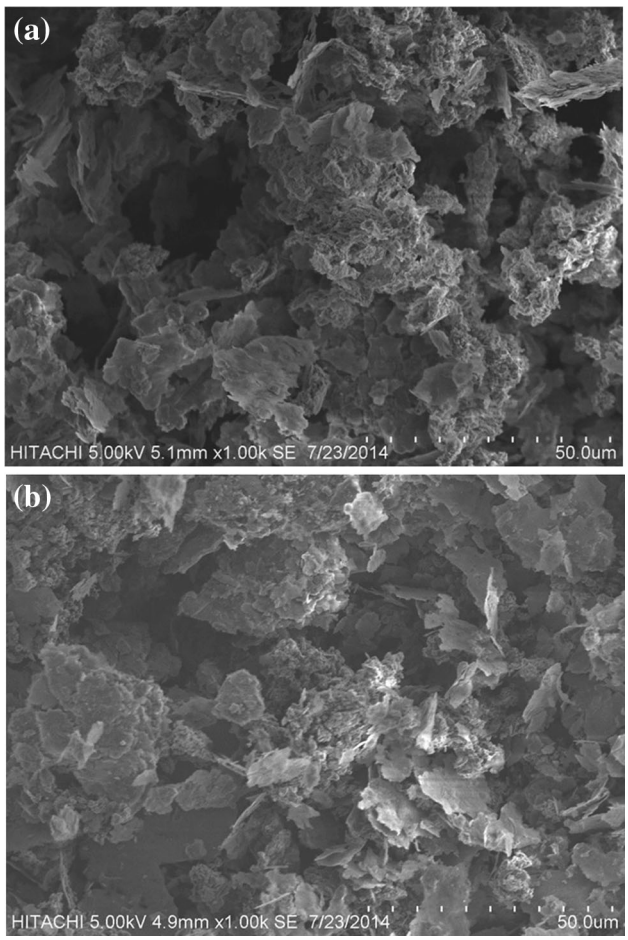

Fig. 5 Morphology of (**a**) Al-5CNTs and (**b**) Al-10CNTs nanocomposite powders milled for 8 h

efficiency of milling time on the dispersion of CNTs. It can be seen that 2 wt.% CNTs are homogenously dispersed after 8 h of milling in steady state (Fig. 7b). The well dispersion of CNTs can be found in Al-1CNTs after 8 h of milling [5]. Interestingly, increasing CNTs content from 2 to 5 and 10 wt.% in the constant milling time of 8 h shows different results. Figure 7c shows that, however, CNTs are shortened, but there are scattered clusters on the surface of aluminum even at long milling time of 8 h. Some scattered clusters of CNTs can be seen on the surface of Al particles in Al-10CNTs even after 8 h of milling as highlighted by circle in Fig. 7c. This demonstrates that 8 h of milling is not long enough to disperse 10 wt.% of CNTs within Al matrix.

Structural Analysis of Ball-Milled Al-Al_2O_3 and Al-CNT Nanocomposites

Ball milling of Al-CNT nanocomposites was found to damage CNTs structure, especially at longer milling times and in the presence of larger CNT contents. The damaged structure of CNTs was revealed according to the Raman spectra of the initial CNT and ball-milled Al-CNT nanocomposites (not shown here). In Al-10CNT nanocomposites, the I_G/I_D ratio progressively decreases from 0.86 at 0.46 by increasing the milling time from 0.5 h to 12 h which implies the damaged CNTs structure during ball milling. The damage of CNTs structure in Al-2CNTs is also previously reported [20]. Each Raman spectra consist of two distinct peaks, which represent a G band due to vibrational modes and a D band arising from disorder-induced modes [20]. The ratio of the intensities of the G and D bands (I_G/I_D) provides an estimation of defect density in the graphitic structures [24]. Therefore, the quantities of defects increase in the CNTs structure particularly at longer milling times.

The damaged CNTs structure results in the formation of unwanted brittle Al_4C_3 phase during subsequent sintering process which has deleterious effect on ductility of Al-CNT nanocomposites [11, 16, 20, 25]. Ball-milled Al-CNT powders are unstable in terms of energy, and sintering process makes them more reactive. However, Al-CNT powders milled for shorter milling times of 0.5 and 2 h seem not to be so unstable at least in terms of activation energy. The x-ray diffraction patterns of Al-2CNT nanocomposites milled for different times confirm the formation of Al_4C_3 phase (Fig. 8). The formation of Al_4C_3 is also reported in authors' previous study [16].

As the CNT contents increase up to 5 wt.%, the formation of Al_4C_3 phase is accelerated so that Al_4C_3 phase is formed at shorter milling times. Figure 9 shows that Al_4C_3 phase is formed after 8 h of milling. By increasing milling time and CNT contents, more damages are induced to CNTs structure. In fact, formation of Al_4C_3 phase facilitates by the crystallographic defects and possible CNTs amorphization during sintering process. Therefore, extending the time of milling could adversely affect the mechanical properties of final nanocomposites due to damaged CNTs structure and presence of impurities, such as Al_2O_3 oxides and Al_4C_3 in the microstructure. However, formation of carbide may increase the bonding between CNTs and Al, thereby improving mechanical strength, but it decreases the ductility of the composite [24, 26].

The formation of Al_4C_3 phase is originated in CNT itself. During milling process, the stability of CNTs is reduced due to the damage of their structure. Therefore, amorphization of CNTs and formation of some supersaturated solid solution of carbon is expected [16]. It should also be noted that the absence of Al_4C_3 peaks in some patterns does not rule out that Al_4C_3 phase is not formed in those nanocomposites. The absence of Al_4C_3 peaks is probably due to the size, structure, and the amount of Al_4C_3 phase which might be out of detector resolution range. As the reinforcement is being refined during milling,

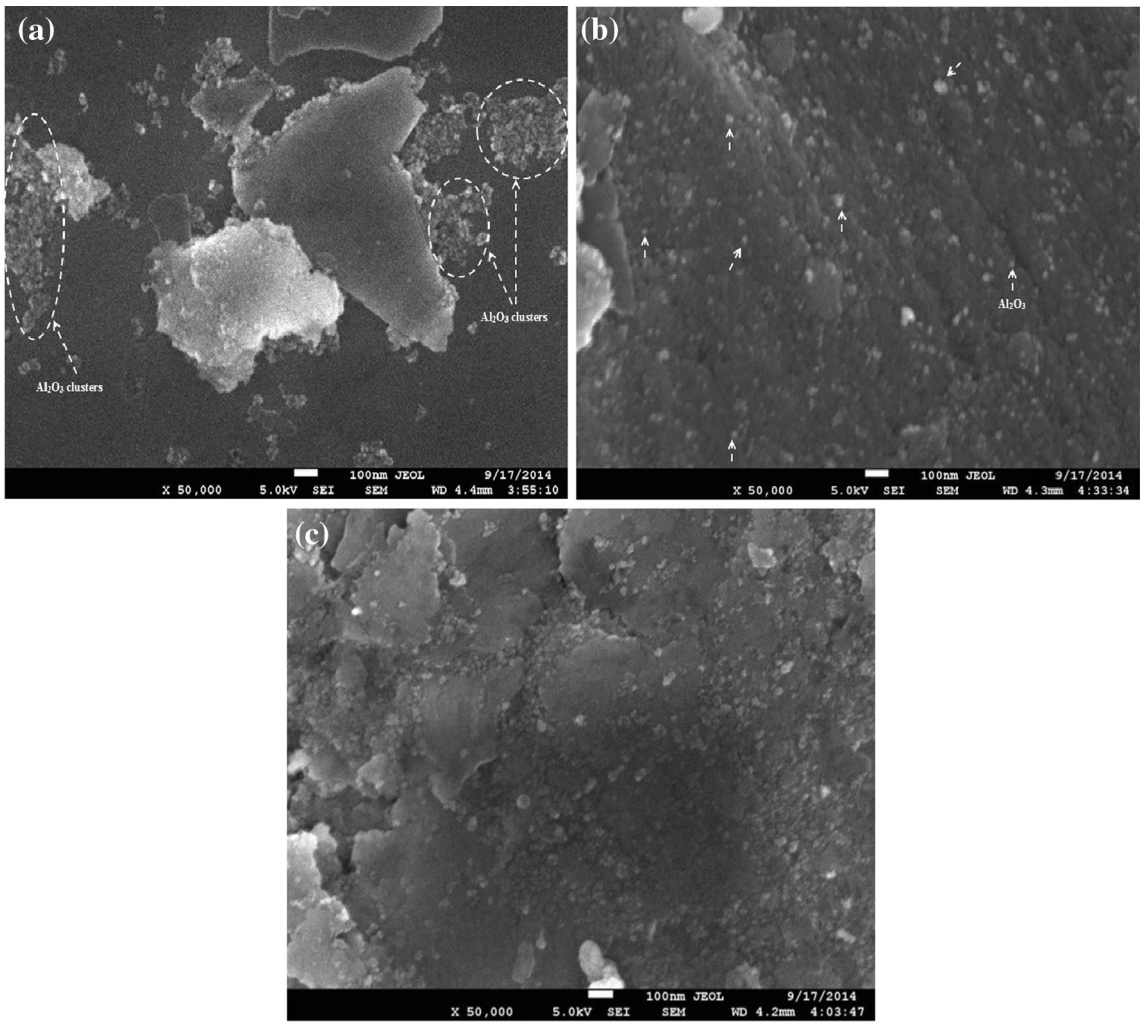

Fig. 6 Dispersion uniformity of Al_2O_3 nanoparticles within pure Al matrix in Al-2Al_2O_3 nanocomposites milled for (**a**) 0.5 h and (**b**) 8 h and (**c**) Al-10Al_2O_3 nanocomposite milled for 8 h

the detection limit of XRD significantly increases so that one cannot decide firmly about the formation of carbides [27]. Figure 10 reveals the presence of Al_4C_3 phase under TEM observation of Al-10CNTs nanocomposite powders milled for 8 h. Needle-shaped Al_4C_3 phase is highlighted in Al-10CNTs microstructure as observed in Al-5CNTs [16]. The formation of needle-shaped Al_4C_3 phase is also reported by Esawi et al. [11] and Kwon et al. [28]. Some CNTs were also found close to the Al_4C_3 phase suggesting that not all of CNTs have reacted with aluminum.

The x-ray diffraction patterns of Al-10Al_2O_3 nanocomposite powders ball-milled for various times are presented in Fig. 11. Neither the presence of unwanted phases nor impurity phases such as Al_4C_3 was revealed from the diffraction pattern even in the presence of large Al_2O_3 nanoparticle contents. The results are in good agreement with previous findings by Zebarjad et al. [29] and Prabhu et al. [30]. The absence of impurity or unwanted phases results in a clean interface between particle and matrix. According to the literature, the Al_2O_3 phase is such stable that no unwanted solid-state reaction occurs during the milling of Al-Al_2O_3 nanocomposite powders [27, 29, 30]. It can be inferred that mechanical milling is appropriate method to disperse hard, small, and equiaxed reinforcements. The less number of Al_2O_3 peaks and low intensity in the diffraction pattern compared to the diffraction peaks from aluminum might be due to low weight fraction of the Al_2O_3 phase and/or the fine size of the powder in the Al-Al_2O_3 powder mixture [30].

Mechanical Properties of Al-Al_2O_3 and Al-CNT Nanocomposites

It is well known that each reinforcement provides various characteristic profiles, while the same composition and amounts of the reinforcements are involved [15]. CNT and

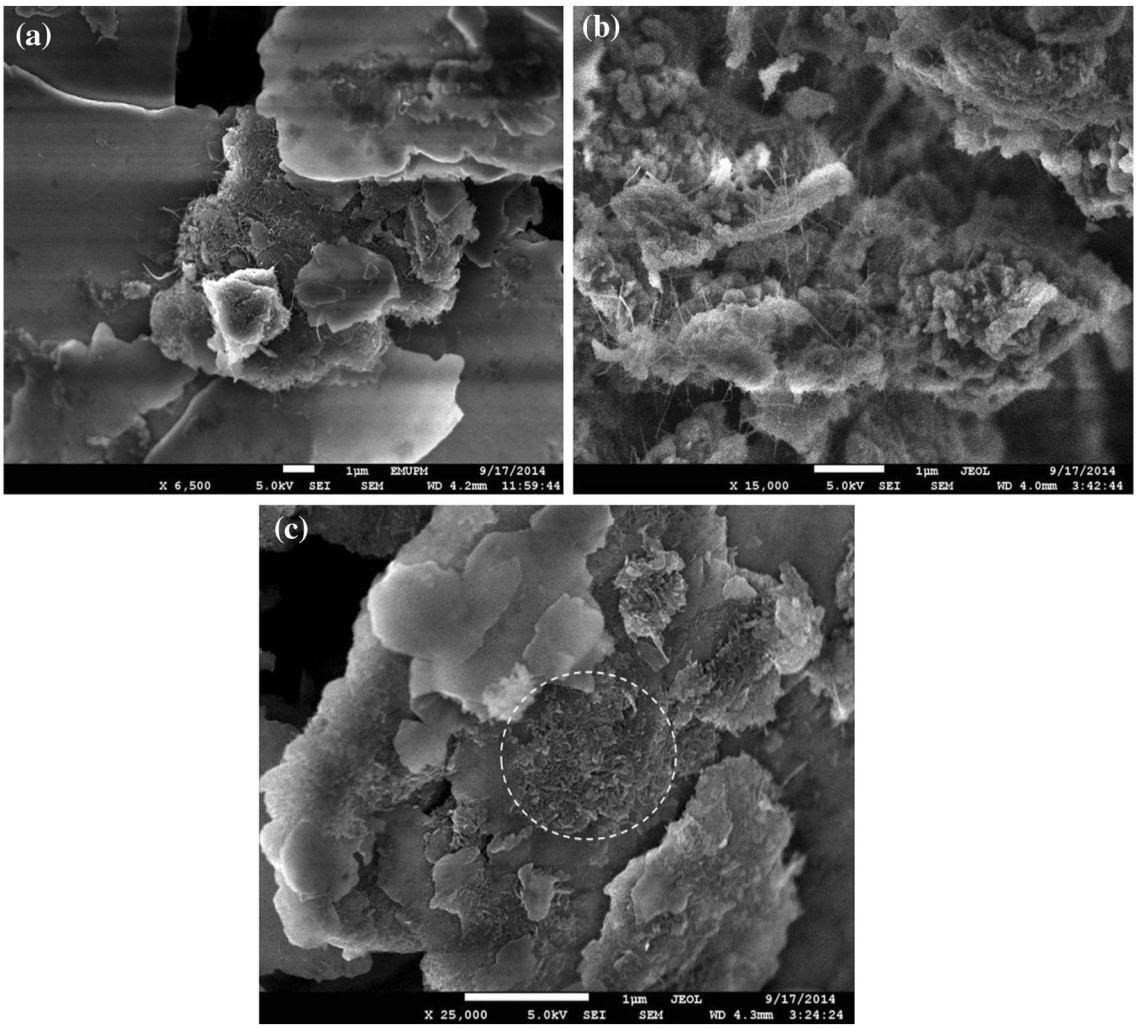

Fig. 7 Dispersion uniformity of CNTs within Al matrix in Al-2CNT nanocomposites milled for (**a**) 0.5 h and (**b**) 8 h and (**c**) Al-5CNTs composite milled for 8 h

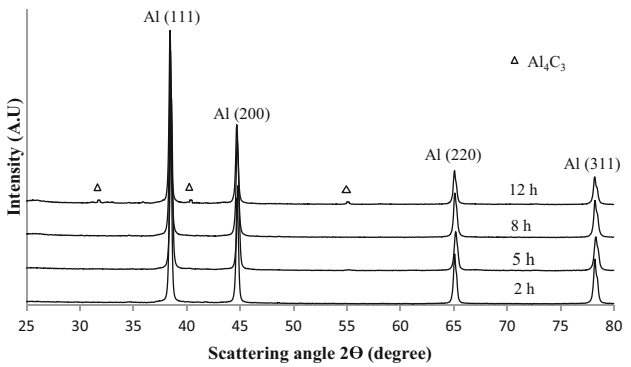

Fig. 8 XRD patterns of Al-2CNT nanocomposites milled for different times

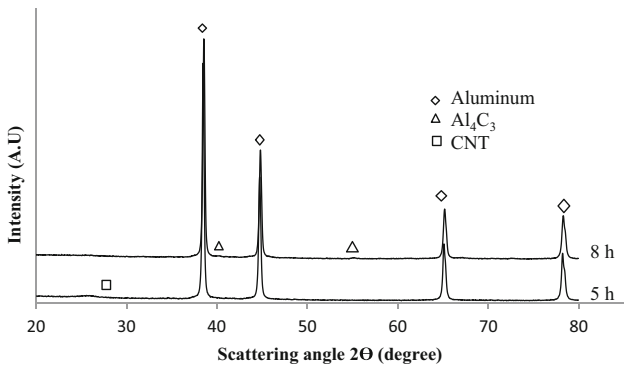

Fig. 9 XRD patterns of Al-5CNTs nanocomposite milled for different times

Al_2O_3 nanoparticles are different in the shape and properties. For example, Young's modulus of CNT is around $\sim$ 1 TPa, while it is $\sim$ 353 MPa for Al_2O_3. Therefore, different mechanical behaviors of Al-Al_2O_3 and Al-CNT nanocomposites are expected.

Nanohardness (HN) and Young's modulus (E) of Al-CNT and Al-Al_2O_3 nanocomposites with different Al_2O_3

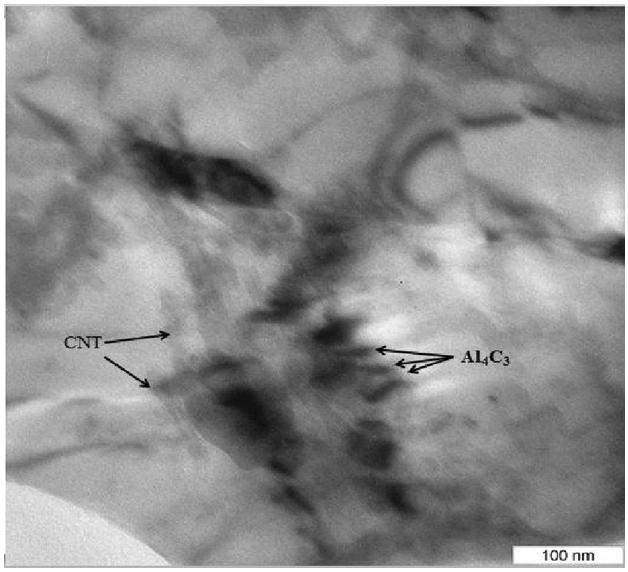

Fig. 10 TEM micrograph of Al-10CNTs nanocomposite powders milled for 8 h showing the formation of Al_4C_3 phase

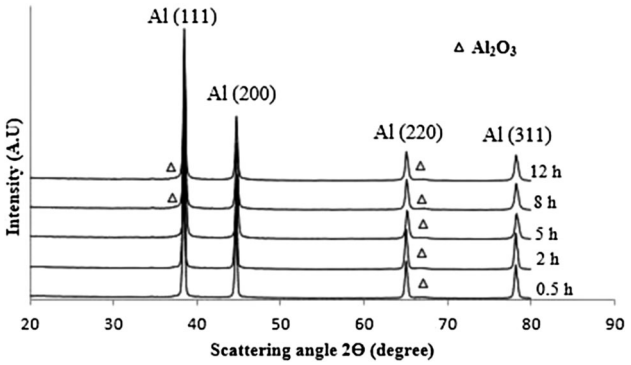

Fig. 11 XRD patterns of Al-10Al_2O_3 nanocomposite powders milled for different times

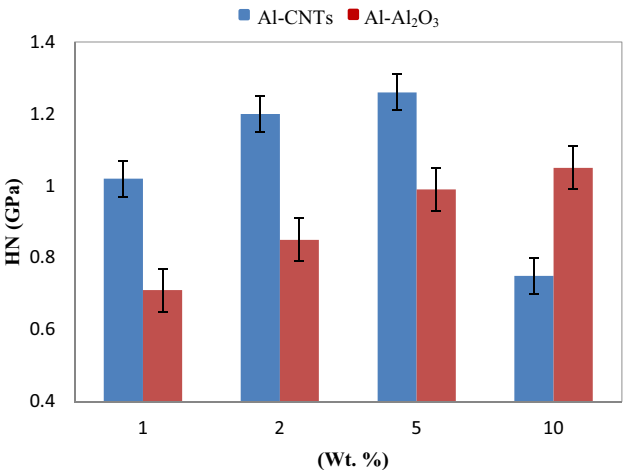

Fig. 12 Nanohardness of Al-CNT and Al-Al_2O_3 nanocomposites milled for 8 h

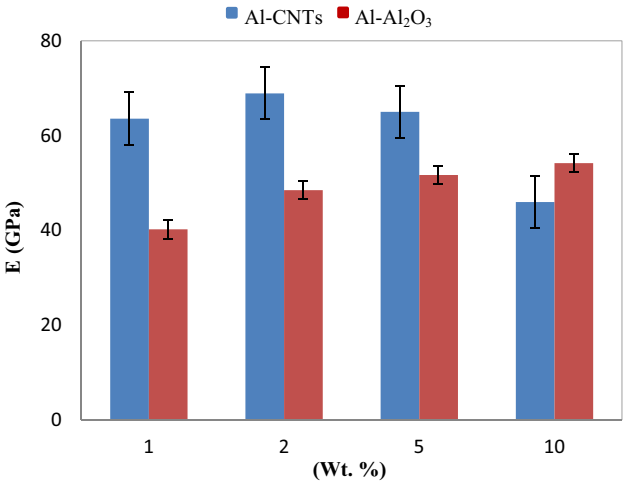

Fig. 13 Young's modulus of Al-CNT and Al-Al_2O_3 nanocomposites milled for 8 h

and CNT contents milled in the steady state are compared in Figs. 12 and 13. It can be observed that when smaller content of Al_2O_3 and CNT reinforcements is used (up to 5 wt.%), HN and E values of Al-CNT nanocomposites are higher than the that of Al-Al_2O_3 nanocomposites. In contrast, HN and E values of Al-10Al_2O_3 nanocomposites are found to be higher than that of Al-10CNT nanocomposites. Large amount of CNTs (10 wt.%) results in a significant drop in the HN and E values of Al-CNT nanocomposites even to a lower values than Al-1CNTs. The drop in mechanical behavior of Al-10CNT nanocomposites can be attributed to poor consolidation which occurs in the presence of CNT clustered areas. Agglomeration of nanocomposite particles and clustering of CNTs in Al-10CNT nanocomposites may interrupt diffusion bonding during sintering processes resulting in the weak bonding of particles and formation of large amount of porosity and cracks in the final nanocomposite [20, 28]. It has been reported that porosity and cracks significantly reduce the measured Young's modulus of metals [31, 32].

In the case of Al-10Al_2O_3 nanocomposites, some agglomerations of particles were formed at longer milling times; however, homogenous dispersion of Al_2O_3 was observed. It seems that the effect of dispersion homogeneity of reinforcements is dominant over their intrinsic properties of Al_2O_3 nanoparticles. The presence of large contents of Al_2O_3 nanoparticles modifies the milling process by accelerating the deformation of particles. However, the interfacial bonding between Al and Al_2O_3 is of concern. There is no interaction between aluminum and Al_2O_3 nanoparticles, and the relatively low wettability of the Al-Al_2O_3 system does not provide strong bonds between particles [33]. On the other hand, Al_2O_3 nanoparticles are more brittle than CNTs and they often display cracks and

porosity around themselves resulting in the weakening of the Al-10Al_2O_3 nanocomposite [34].

The variations of increment of HV and E values of milled Al-CNT and Al-Al_2O_3 nanocomposites are related to the presence of CNT and Al_2O_3 nanoparticles and deformed structure resulting from milling process [11, 16, 20, 21, 35]. The main contribution to improved mechanical behavior of Al-CNT and Al-Al_2O_3 nanocomposites is the homogenous dispersion of CNT and Al_2O_3 nanoparticles along with grain refining within milling, less interparticle spacing, good and tight interfacial bonding between nanoparticles and matrix and less amount of porosities [16, 20, 21]. The enhancement in mechanical behavior of Al-CNT and Al-Al_2O_3 nanocomposites are empowered by in formation of high dislocation density. The interaction of CNT and Al_2O_3 nanoparticles with Al particles results in formation of high dislocation density which leads further grain refining [35].

Conclusions

In this study, morphological, microstructural features and mechanical behavior of Al-Al_2O_3 and Al-CNT nanocomposites powders were compared. The outcomes of this study are as follow:

1. Most of Al-CNT and Al-Al_2O_3 nanocomposites were found to reach steady state after 8 of milling except Al-5CNT and Al-10CNTs which never reached steady state due to the formation of big agglomerates resulting in non-homogenous nanocomposite powders.
2. Ball milling was found to be an effective technique to disperse CNT (at lower amounts) and Al_2O_3 nanoparticles (even at high amount) homogenously within Al matrix. It was also found that ball milling even at longer milling times up to 12 h is not sufficient to disperse CNT contents larger than 2 wt.%.
3. Formation of carbide phase (Al_4C_3) was observed for Al-CNT nanocomposites containing CNT contents larger than 5 wt.% CNTs and longer milling times as a result of reaction of carbon with aluminum matrix. However, no chemical reaction between Al matrix and Al_2O_3 nanoparticles was observed.
4. It was found that mechanical behavior of Al-CNT and Al-Al_2O_3 nanocomposites improves significantly with the addition of CNT and Al_2O_3 nanoparticles. Generally, hardness and Young's modulus of Al-CNT nanocomposites were higher than Al-Al_2O_3 nanocomposites. An exception was observed in the comparison of Al-10CNT with Al-10Al_2O_3 nanocomposites.

Acknowledgments The authors would like to thank Associated Professor Khamirul Amin Matori for his academic support given throughout this research work.

References

1. M.K. Surappa, Aluminium matrix composites: challenges and opportunities. Sadhana. **28**(1), 319–334 (2003)
2. J.M. Torralba, C.E. Da Costa, F.J. Velasco, P/M aluminum matrix composites: an overview. J. Mater. Process. Tech. **133**(1–2), 203–206 (2003)
3. K.U. Kainer, *Metal matrix composites: custom-made materials for automotive and aerospace engineering* (Wiley, New York, 2006)
4. R. Casati, M. Vedani, Metal matrix composites reinforced by nanoparticles—a review. Metals **4**, 65–83 (2014)
5. F. Ostovan, K.A. Matori, M. Toozandehjani, A. Oskoueian, H.M. Yusoff, R. Yunus, A.H.M. Ariff, Microstructural evaluation of ball-milled nano Al_2O_3 particulate-reinforced aluminum matrix composite powders. Int. J. Mater. Res. **106**(6), 636–640 (2015)
6. M.K. Aghajanian, R.A. Langensiepen, M.A. Rocazella, J.T. Leighton, C.A. Andersson, The effect of particulate loading on the mechanical behaviour of Al_2O_3/Al metal-matrix composites. J. Mater. Sci. **28**(24), 6683–6690 (1993)
7. S.M. Zebarjad, S.A. Sajjadi, Dependency of physical and mechanical properties of mechanical alloyed Al-Al_2O_3 composite on milling time. Mater. Des. **28**(7), 2113–2120 (2007)
8. Y.C. Kang, S.L.I. Chan, Tensile properties of nanometric Al_2O_3 particulate-reinforced aluminum matrix composites. Mater. Chem. Phys. **85**(2), 438–443 (2004)
9. A.M.K. Esawi, K. Morsi, A. Sayed, A.A. Gawad, P. Borah, Fabrication and properties of dispersed carbon nanotube-aluminum composites. Mater. Sci. Eng. A **508**(1), 167–173 (2009)
10. A.M.K. Esawi, K. Morsi, Dispersion of carbon nanotubes (CNTs) in aluminum powder. Compos. A Appl. Sci. Manuf. **38**(2), 646–650 (2007)
11. A.M.K. Esawi, K. Morsi, A. Sayed, M. Taher, S. Lanka, Effect of carbon nanotube (CNT) content on the mechanical properties of CNT-reinforced aluminum composites. Compos. Sci. Tech. **70**(16), 2237–2241 (2010)
12. R. Perez-Bustamante, I. Estrada-Guel, W. Antunez-Flores, M. Miki-Yoshida, P.J. Ferreira, R. Martinez-Sanchez, Novel Al-matrix nanocomposites reinforced with multi-walled carbon nanotubes. J. Alloy. Compound. **450**(1–2), 323–326 (2008)
13. S.R. Bakshi, A. Agarwal, An analysis of the factors affecting strengthening in carbon nanotube reinforced aluminum composites. Carbon **49**(2), 533–544 (2011)
14. C. Suryanarayana, N. Al-Aqeeli, Mechanically alloyed nanocomposites. Prog. Mater Sci. **58**(4), 383–502 (2013)
15. H. Uozumi, K. Kobayashi, K. Nakanishi, T. Matsunaga, K. Shinozaki, H. Sakamoto, M. Yoshida, Fabrication process of carbon nanotube/light metal matrix composites by squeeze casting. Mater. Sci. Eng. A **495**(1–2), 282–287 (2008)
16. F. Ostovan, K.A. Matori, M. Toozandehjani, A. Oskoueian, H.M. Yusoff, R. Yunus, A.H.M. Ariff, H.J. Quah, W.F. Lim, Effects of CNTs content and milling time on mechanical behavior of MWCNT-reinforced aluminum nanocomposites. Mater. Chem. Phys. **166**(15), 160–166 (2015)
17. F. Tang, I.E. Anderson, S.B. Biner, Solid state sintering and consolidation of Al powders and Al matrix composites. J. Light Met. **2**(4), 201–214 (2002)
18. J.B. Fogagnolo, F. Velasco, M.H. Robert, J.M. Torralba, Effect of mechanical alloying on the morphology, microstructure and

properties of aluminum matrix composite powders. Mater. Sci. Eng. A **342**(1), 131–143 (2003)
19. C. Suryanarayana, Mechanical alloying and milling. Prog. Mater Sci. **46**(1), 1–184 (2001)
20. F. Ostovan, K.A. Matori, M. Toozandehjani, A. Oskoueian, H.M. Yusoff, R. Yunus, A.H.M. Ariff, Nanomechanical behavior of multi-walled carbon nanotubes particulate reinforced aluminum nanocomposites prepared by ball milling. Materials. **9**(3), 140 (2016)
21. Toozandehjani, M., Matori, K.A., Ostovan, F., Sidek, A.A. Shuhazlly M.M.: Effect of milling time on the microstructure, physical and mechanical properties of Al-Al_2O_3 nanocomposite synthesized by ball milling and powder metallurgy. Materials. 10. (2017)
22. W.C. Oliver, G.M. Pharr, An improved technique for determining hardness and elastic modulus using load and displacement sensing indentation. J. Mater. Res. **7**(06), 1564–1583 (1992)
23. B. Xiong, Z. Xu, Q. Yan, B. Lu, C. Cai, Effects of SiC volume fraction and aluminum particulate size on interfacial reactions in SiC nanoparticulate reinforced aluminum matrix composites. J. Alloy. Compound. **509**(4), 1187–1191 (2011)
24. K.E. Thomson, D. Jiang, R.O. Ritchie, A.K. Mukherjee, A preservation study of carbon nanotubes in alumina-based nanocomposites via Raman spectroscopy and nuclear magnetic resonance. Appl. Phys. A **89**(3), 651–654 (2007)
25. J.S. Benjamin, M.J. Bomford, Dispersion strengthened aluminum made by mechanical alloying. Metall. Trans. A **8**(8), 1301–1305 (1997)
26. J.H. Ahn, Y.J. Kim, S.S. Yang, Multiwall carbon nanotube reinforced aluminum matrix composites prepared by ball milling. Appl. Mech. Mater. **372**, 119–122 (2013)
27. H. Ahamed, V. Senthilkumar, Role of nano-size reinforcement and milling on the synthesis of nano-crystalline aluminium alloy composites by mechanical alloying. J. Alloy. Compound. **505**(2), 772–782 (2010)
28. H. Kwon, M. Saarna, S. Yoon, A. Weidenkaff, M. Leparoux, Effect of milling time on dual-nanoparticulate-reinforced aluminum alloy matrix composite materials. Mater. Sci. Eng. A **590**, 338–345 (2014)
29. S.M. Zebarjad, S.A. Sajjadi, Microstructure evaluation of Al-Al_2O_3 composite produced by mechanical alloying method. Mater. Design. **27**(8), 684–688 (2006)
30. B. Prabhu, C. Suryanarayana, L. An, R. Vaidyanathan, Synthesis and characterization of high volume fraction Al-Al_2O_3 nanocomposite powders by high-energy milling. Mater. Sci. Eng. A **425**(1), 192–200 (2006)
31. X.C. Zhang, B.S. Xu, F.Z. Xuan, S.T. Tu, H.D. Wang, Y.X. Wu, Porosity and effective mechanical properties of plasma-sprayed Ni-based alloy coatings. Appl. Surf. Sci. **255**(8), 4362–4371 (2009)
32. C.N. He, N.Q. Zhao, C.S. Shi, S.Z. Song, Mechanical properties and microstructures of carbon nanotube-reinforced Al matrix composite fabricated by in situ chemical vapor deposition. J. Alloy. Compound. **487**(1), 258–262 (2009)
33. K.M. Shorowordi, T. Laoui, A.S.M.A. Haseeb, J.P. Celis, L. Froyen, Microstructure and interface characteristics of B_4C, SiC and Al_2O_3 reinforced Al matrix composites: a comparative study. J. Mater. Process. Technol. **142**(3), 738–743 (2003)
34. M. Kouzeli, L. Weber, C. San Marchi, A. Mortensen, Influence of damage on the tensile behavior of pure aluminum reinforced with $\geq$ 40 vol pct alumina particles. Acta Mater. **49**(18), 3699–3709 (2001)
35. A.A. Mazilkin, M.M. Myshlyaev, Microstructure and thermal stability of superplastic aluminium-lithium alloy after severe plastic deformation. J. Mater. Sci. **41**(12), 3767–3772 (2006)